A High Efficiency Gas Phase Photoreactor for Eradication of Methane from Low-Concentration Sources

Morten Krogsbøll[1], Hugo S. Russell[1,2] and Matthew S. Johnson[1,3,*]

[1] Ambient Carbon ApS, Forhaabningsholms Alle 19, 1.th, DK-1904 Frederiksberg C, Denmark.
[2] Aarhus University, Department of Environmental Science, Frederiksborgvej 399, DK-4000 Roskilde, Denmark
[3] University of Copenhagen, Department of Chemistry, Universitetsparken 5, DK-2100 Copenhagen OE, Denmark
*Corresponding Author

E-mail: msj@chem.ku.dk

Abstract.

Despite the urgent need, very few methods are able to efficiently remove methane from waste air with low cost and energy per unit volume, especially at the low concentrations found in emissions from e.g. wastewater treatment, livestock production, biogas production and mine ventilation. We present the first results of a novel method based on using chlorine atoms in the gas phase, thereby achieving high efficiency. A laboratory prototype of the Methane Eradication Photochemical System (MEPS) technology achieves 58% removal efficiency with a flow capacity of 30 L/min; a reactor volume of 90 L; UV power input at 368 nm of 110 W; chlorine concentration of 99 ppm; and a methane concentration of 55 ppm; under these conditions the apparent quantum yield (AQY) ranged from 0.48 to 0.56% and the volumetric energy consumption ranged from 36 to 244 kJ/m^3. The maximum achieved AQY with this system was 0.83%. A series of steps that can be taken to further improve performance are described. These metrics show that MEPS has the potential to be a viable method for eliminating low-concentration methane from waste air.

Keywords: Photoactivation, Chlorine Radicals, Methane Removal, Agricultural Methane Emissions, Gas Phase Oxidation, Methane Control

Submitted to: *Environ. Res. Lett. - Focus on Methane Drawdown*

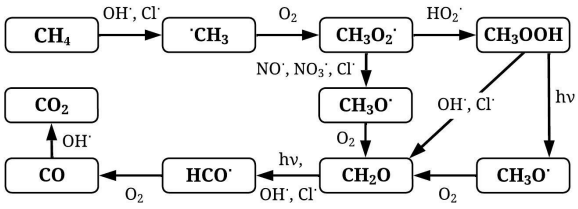

Figure 1. The main processes in the gas phase oxidation of methane at ambient temperature, based on radical chain reactions, for nominal atmospheric and high chlorine conditions.

1. Introduction

Methane is a greenhouse gas and plays a key role in atmospheric chemistry, the formation of air pollution and the atmosphere's oxidation capacity [1]. Between 1750 and 2022, the atmospheric methane concentration has risen from 729±10 ppb to 1910 ppb [2, 3]. Methane alone has increased anthropogenic radiative forcing by 1.19±0.39 W/m^2, which is responsible for a 0.6 [0.3-1.0] °C increase in global mean surface air temperature [4].

A significant amount of anthropogenic methane emissions, ∼40%, are from the agricultural sector [4], where animal production in particular makes a large contribution [5]. Methane sinks include methanotrophs in the soil (∼10%) and gas phase radical reactions, mainly with the OH radical per reaction 1.

$$CH_4 + OH^{\bullet} \quad \rightarrow \quad {}^{\bullet}CH_3 + H_2O \qquad (1)$$

Where $k(298\ \mathrm{K}) = 6.5{\pm}0.5{\times}10^{-15}\ \mathrm{cm^3\ molecule^{-1}\ s^{-1}}$ [6, 7]. Atomic chlorine, Cl$^{\bullet}$, removes a few percent by reaction 2 [5, 8, 9, 10].

$$CH_4 + Cl^{\bullet} \quad \rightarrow \quad {}^{\bullet}CH_3 + HCl \qquad (2)$$

Where $k(298\ \mathrm{K}) = 1.05{\pm}0.05{\times}10^{-13}\ \mathrm{cm^3\ molecule^{-1}\ s^{-1}}$ [11, 12]. Both of these reactions lead to the formation of CO_2 through the oxidation path shown in figure 1, where radicals play an important role in multiple steps of the oxidation.

A limited number of technologies are available for point source emissions control of methane. For the oxidation of higher concentration methane streams (1000 ppm to 44,000 ppm), there are commercialized methods that can operate at scale, e.g., Regenerative Thermal Oxidation (RTO), and Catalytic Thermal Oxidation (CTO) [13]. They operate by oxidizing pollution with heat, or by running the air stream over a catalyst bed at elevated temperatures. Due to the capital and operating costs, the RTO method is suited to high levels of VOCs including methane (above 0.1-0.2%) in large air flows such as might be found in industrial settings [14]. Low-concentration methane sources can be treated, but at prohibitively high cost and energy input. RTO will also produce NOx gases due to the high temperatures needed for effective methane removal. For CTO methods, the main costs are due to the increase in temperature and the size required for large air flows to gain the needed residence time over the catalyst [15]. For agricultural and wastewater treatment conditions working with flows at a scale of m^3/s, these approaches would require unreasonably large systems. The minimum concentration for methane removal demonstrated in a laboratory for CTO is 200 ppm as reported by Gélin et al.[15]. Industrial thermal and catalytic oxidisers typically have a high thermal efficiency, ca. 95% [16]. At a typical operating temperature of 1000 °C this implies a heat loss corresponding to a change in temperature of the airstream of 50 K. Taking the specific heat capacity of air ∼1 J/(g K) and the density of air ∼1.2 kg/m^3, this means the specific power requirement is ∼60 kJ/m^3. Thermal and catalytic oxidisers may not be suitable for some applications due to the need for addition of natural gas to keep the combustion bed hot, their cost, and the fact that they work best for stable pollution loads whereas many industrial processes are intermittent.

A recent paper by Abernethy et al. [17] has assessed methane oxidation technologies using a concentration based framework. This paper estimates, for the first time, the amount of methane emitted at a given concentration, showing that around 3/4 of methane emissions occur at a concentration below 1000 ppm.

Emerging methods for the oxidation of low-level methane include biofilters [18], photocatalysts [19], and catalysts combined with zeolites [20]. However, thus far none of these have been proven at scale with an acceptable volumetric (kJ/m^3) or specific (kJ/kg) energy input [20, 21].

Methane is chemically inert and many of its physical properties (molecular weight, critical temperature, boiling point, ionization energy, proton affinity) fall in

the range of those of the noble gases He, Ne, Ar, Kr and Xe [22]; a table with the values can be found in the supporting material. This means that methane interacts weakly with surfaces, and has only a very weak physisorption interaction. The low affinity of methane for surfaces interferes with the efficiency of catalytic oxidation of methane, and it also makes it difficult to capture methane using an adsorbant such as activated charcoal, zeolites or MOFs. One breakthrough could come in the form of carbohydrates that form clathrate type adducts with methane [23]. Finally, methane is weakly soluble in water, making separation with scrubbers very inefficient, and also creating a mass transfer barrier for biological treatment methods using methanogenic bacteria.

The introduction of gas phase advanced oxidation (GPAO) [24, 25] provides a way of overcoming some of the limitations of these existing technologies. GPAO systems operate by producing reactive radical species in-situ through the use of precursors photolyzed by UV lights. These then react rapidly with the target species in the gas phase. OH radicals can be produced by photolysis of ozone from an ozone generator using oxygen and humidity present in the air [25]. This approach improves upon other methods in the following ways. First, since reactions occur in the gas phase and not on a solid surface, there is a significant reduction in pressure drop. Resistance to air flow is often one of the largest terms in the energy budget, especially for low pollutant concentrations. Second, GPAO operates at ambient temperatures, eliminating energy used to heat a catalyst bed or cycle an adsorbent. Third, GPAO is a simple robust system that doesn't have the capital costs associated with a catalyst bed and rare earth elements. Fourth, low specific and volumetric energy input can be achieved because treatment occurs at the temperature of the airstream and with a low pressure drop.

Unfortunately, due to the low reaction rate coefficient of reaction 1, OH is difficult to utilize for methane control at scale, as there is an inherent limitation of the space velocity; the long treatment time of the method would require unreasonably large systems [25]. In the case of methane the issue of long treatment time (i.e. limited space velocity requiring a large reactor) cannot be overcome using more UV lamps or more radical precursor. The system operates near the OH saturation concentration determined by the reaction of OH with its precursor (OH + O_3), it's self reaction (OH + OH) and reaction with other radicals in the system (e.g. OH + HO_2).

A chlorine based system [26, 27], as shown in figure 2, would overcome these limitations in several ways. First, reaction 2 is ∼15 times faster than reaction 1. Second, it requires less energy to generate

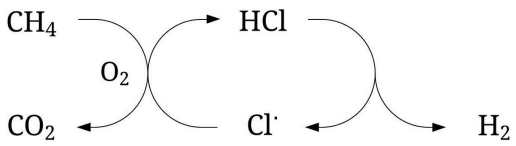

Figure 2. In MEPS, hydrogen is pumped from methane to molecular hydrogen with a chloride cycle interconverting chloride (Cl^{-1}) and chlorine (Cl^0).

Cl radicals than OH radicals, due to the different wavelengths needed to photolyze O_3 and Cl_2, as well as the proportion of O_3 photolyzed that does not generate OH radicals [28]. Third, a higher concentration of Cl can be maintained compared to OH. The saturation point is much higher in a chlorine based system because the three body recombination of two atoms, Cl + Cl + M → Cl_2 + M is very slow [29], and if it does form it does not accumulate as it will quickly be photolysed by the UV light. In a chlorine based system, it is necessary to include a method for capturing the chloride product and recycling it back to chlorine in order to lower raw material costs and prevent the release of chlorine-containing byproducts. This chlorine based technology was first introduced as a method to remove interference from ambient methane in spectroscopy of gases in ice core samples, by Polat et al. (2021) [27].

We present the first full description of a Methane Eradication Photochemical System (MEPS) for methane mitigation. We have demonstrated MEPS at 50 ppm methane with a flow rate of 30 L/min, which is ∼4000 times higher than that demonstrated by Polat et al. (2021). Moreover, the specific energy demand of this work is ∼3500 times lower than the specific energy reported by Polat et al. (2021). The work presented in this paper is described in patent filing WO2022053603A1 (2022) and related documents [26].

2. Method

A laboratory scale prototype was constructed as shown in figure 3. Dry, filtered air is added through a 6 mm Teflon tube and then into a 0.9 L mixing tube, from which it enters the reaction chamber. The reaction chamber consists of a 1 m long galvanized steel duct with a 30 x 34 cm cross-section. The duct is lined with polished aluminium covered by a perfluoroalkoxy (PFA) film from Holscot Europe; this combination was found to combine UV reflectivity and resistance to corrosion. The reactor is illuminated from both ends by banks of light emitting diodes with maximum emission at a wavelength of 368 nm (Luminus SST-10-UV-A130-E365-00). Four printed circuit boards each containing 9 LEDs are mounted at each end of the chamber giving 72 LEDs in all. A variable DC power supply was used to power each set of 4 PCBs. The methane is dis-

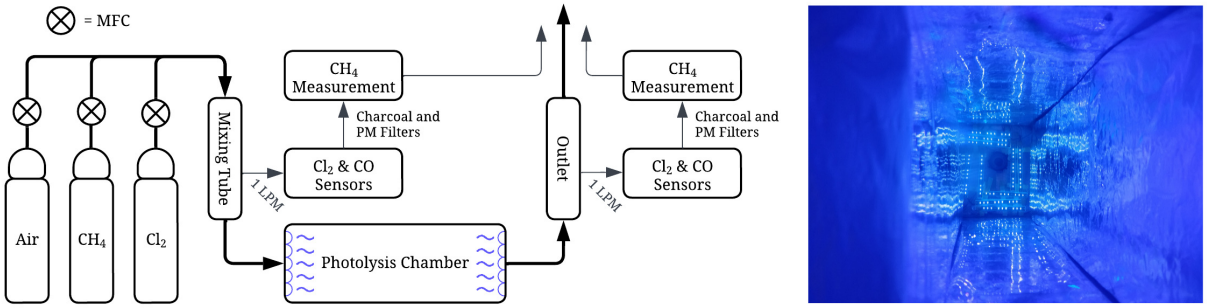

Figure 3. Flow chart of the laboratory setup. The main flow is shown with the larger black arrows. The smaller grey arrows show the measurement streams. The gas input is controlled with mass flow controllers (MFCs). The photolysis chamber has a volume of 90 L, and can be seen with the lights on in the photo on the right.

pensed into the mixing tube through a 6 mm tube from a 100% methane bottle, via a Mass Flow Controller (MFC). The methane concentration is monitored by an Tunable Diode Laser Spectrometer (TDLS) (Axetris LGD Compact-A CH4), one each at the inlet and outlet of the reaction chamber. The chlorine is added to the mixing tube through a 6 mm tube, from a 99.8% chlorine bottle (Air Liquide) with a needle valve. The chlorine concentration is monitored by electrochemical sensors (Membrapor Chlorine Gas Sensor Cl2/C-200) at the inlet and outlet of the reaction chamber. The sensor and data logging system was built by Devlabs ApS of Copenhagen.

At the outlet, the air is directed through a wet scrubber to remove residual Cl_2 and HCl product. The scrubber is comprised of sodium hydroxide solution (20 wt%) trickling over quartz glass Raschig rings. The outlet air flows up through the column. The chlorine concentration was measured at the outlet of the scrubber, with the previously mentioned Cl_2 sensor, to ensure the removal of chlorine (>99%).

The standard operating conditions for the laboratory tests were a total flow of 30 L/min; chlorine concentration of ∼100 ppm; methane ∼50 ppm; and total light power of 110 W. An example time series, figure 4, shows how the relevant concentrations change when the lights are activated.

The methane and chlorine sensors were calibrated using 49.9 ppm and 102.1 ppm gas flasks (Air Liquide), respectively. Calibration gas and dry air were introduced to a 21 L high-density polyethylene calibration chamber via MFCs, with a total flow of ∼5 L/min. The chamber contained 3 mixing fans in X, Y, and Z directions, and a 38 mm PVC outlet tube where multiple sensors could sample via 6 mm Teflon lines. The sensors were calibrated at four different concentrations from 0 to the maximum concentration of the calibration gas flask.

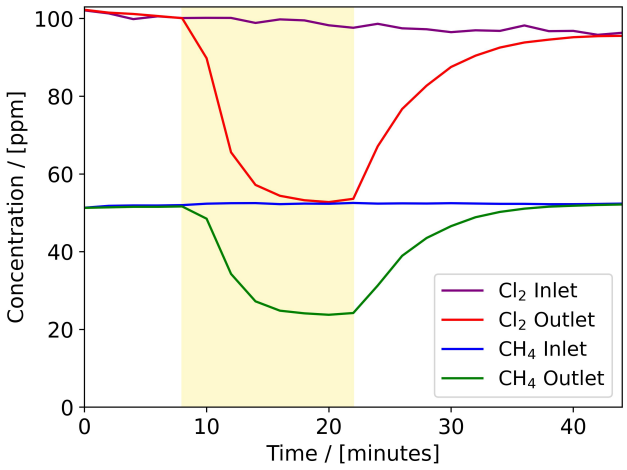

Figure 4. Time series showing how methane and chlorine concentrations at the outlet of the system fall compared to the inlet concentrations when the LEDs are switched on (yellow overlay). In this example, 54% of the methane is oxidized and 48% of the chlorine is photolyzed.

3. Results and Discussion

Under the standard conditions described above, the removal efficiency (RE) for methane in the test reactor was 58±4%; an example is shown in figure 4. The 58% RE under standard conditions and up to 70-80% RE under more favorable Cl_2:CH_4 ratios (shown in figure 5 and in the supporting material) demonstrate the potential of this technology at lab-scale, with dramatic improvements in RE during iterative lab testing.

The key parameters that alter methane RE are the inlet methane and chlorine concentrations, which define the Cl_2:CH_4 ratio, and the light power, which alters the percentage of chlorine that is photolyzed

and available for reaction with methane, thereby altering the Cl:CH_4 ratio. The impact of altering these parameters compared to the standard conditions was investigated in the photoreactor setup by varying the methane concentration between $25 - 55$ ppm; chlorine $43 - 127$ ppm; and light power $18 - 119$ W. In total, 18 tests were conducted (some of which were duplicates using the same conditions). A summary of the individual test conditions can be found in the supporting material.

The impact of all three of these parameters can be summarized by plotting the Cl:CH_4 ratio against RE, while other parameters not mentioned are kept constant. This takes into account the inlet concentrations as well as the amount of Cl_2 that is photolyzed to Cl and is available for reaction with CH_4. This is shown in figure 5. The amount of chlorine radicals produced is calculated by measuring Cl_2 at the inlet and outlet, from which we can see how much chlorine is removed in the process, as some radicals recombine, this is a lower limit for the amount of chlorine radicals produced. As can be seen from the figure, the methane RE increases with the [Cl]:[CH_4] ratio, and under the conditions tested, there is a linear relation between them, with an R^2 value of 0.91, as shown in figure 5. Under the conditions tested, the amount of chlorine radicals created and the amount of methane removed is directly correlated; the relation is linear in the region shown in the figure. We expect however that the system will approach the 100% RE limit asymptotically at Cl:CH_4 ratios greater than 3.

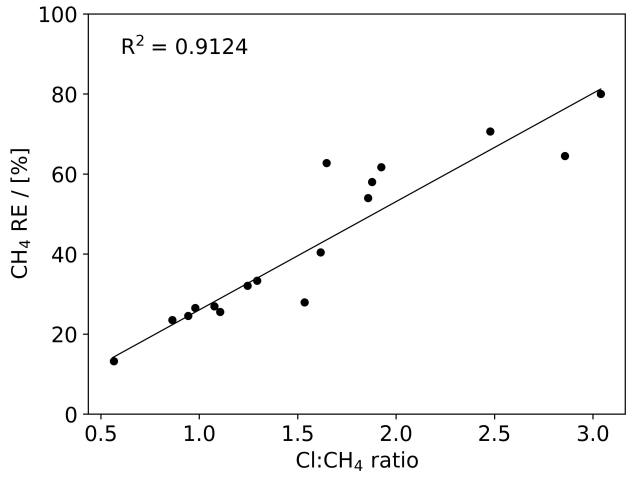

Figure 5. Scatter-plot showing the methane removal efficiency as a function of ratio of the flows (mole/s) of chlorine to methane, 'Cl:CH_4 ratio'. The line is a linear regression fit to the data points.

The energy cost of removing methane (specific energy, J/g) is calculated from the mass of methane removed per minute (using concentration, flow, and RE%), compared with the electrical power. The key terms in the energy budget are chlorine generation (in larger-scale systems, electrolysis will be used to generate chlorine instead of a chlorine bottle); light power; scrubber power; and total flow generation. For the energy calculations in our experiments, scrubber power and total flow generation was found to be low and therefore not included. The light power input was measured, and the chlorine electrolysis power was assumed to be 4 kWh/kg as per the electrolysis device manufacturer, Prominent[30].

The correlation of specific energy with RE shows two important effects. When examining the two low cost quadrants of figure 6, we see that as the light power is increased (red to blue), the RE increases, but so does the energy per mass of methane removed. The RE also depends on the ratio of Cl_2 to CH_4 (small to large circle diameter). Better returns on energy input were found by increasing the Cl_2 concentration relative to light power, as the electrolysis process for producing chlorine is more effective than the photolysis process, at the chlorine concentration and light power we have investigated so far. The relation can be seen as when the light power is kept at 110 W (blue) and the Cl_2:CH_4 ratio (size) is increased, the RE increases and the electricity cost decreases. This is because at higher Cl_2 concentrations, the incident light is absorbed more efficiently, and less is lost to absorption by the reactor walls. This relation is shown by the data-point size and color relative to its position in figure 6. Increasing the volume of the reactor will increase the absorption path length and reduce light and radical loss to the walls. Similarly, increasing the reflectivity of the wall materials will decrease light loss. These changes will be incorporated in future reactor models.

Changes to the reactor volume and total flow will also affect the residence time and thereby the single-pass RE, however, these variables were not investigated in this study.

The specific energy use of the lab-scale system is 2.1-7.7 kWh/g of methane which is a volumetric energy consumption of 36-244 kJ/m^3. We expect the volumetric and specific energy input to further decrease, along with increased RE, due to expected improvements including increasing the reactor volume, using more reflective side wall materials, and removing non-reflective equipment from the reactor. Other potential improvements include the anticipated development of low cost, robust, powerful, high plug efficiency light sources at shorter wavelengths, optimization of heat management (mainly from LEDs) and recycling, changes to the Cl_2:CH_4 ratio, and utilizing the hydrogen produced in electrolysis to generate energy.

To calculate the apparent quantum yield, (methane molecule oxidized per photon), the amount of

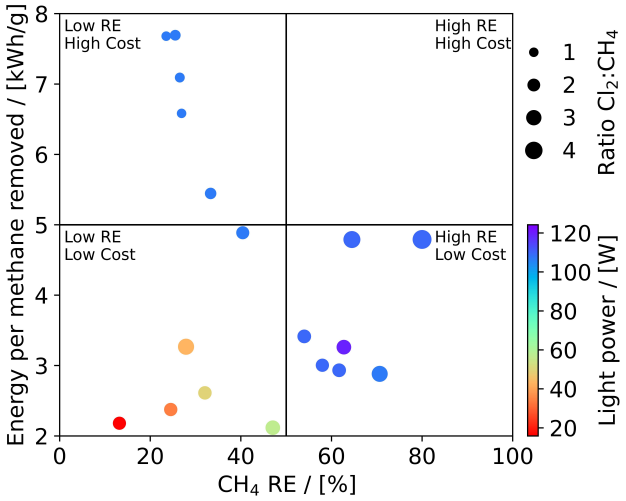

Figure 6. Scatter-plot comparing specific energy to methane RE, with point color varying according to light power and point size with inlet Cl_2:CH_4 ratio.

photons generated have been estimated, using the plug efficiency given by the manufacturer, 35%[31]. That is done using equation 3, where n_{CH_4} is the amount of CH_4 molecules oxidized, e is the plug efficiency of the light source and P_{input} is the power input to the light source.

$$Q_{yield} = \frac{n_{CH_4}}{e \cdot P_{input} \cdot \frac{\lambda}{hc}} \quad (3)$$

The apparent quantum yield ranges from 0.21 to 0.83% depending on conditions.

Further testing will determine performance for specific abatement scenarios. Enclosed cow barns and pig barns are of interest, with methane concentrations of ∼50 ppm, and wastewater treatment plant ventilation systems at ∼300 ppm [32]. The efficiency will also depend on total airflow and potential contaminants in the air stream. Subsequent to the lab-scale prototype tests, a larger field prototype will be tested in these environments before the design is scaled up to a full-size pilot.

A chemical kinetics model has been built; a flowchart of the carbon-containing reactions can be found in the supporting material. The concentrations and global warming potentials of selected species are shown in table 1, species that might raise concern when oxidizing methane using chlorine has been selected and displayed. The ozone depletion potentials (ODPs) of CH_3Cl, CH_2Cl_2 and $CHCl_3$ are all between 0.01 and 0.03 [33], whereas CCl_4 has an ODP of 1.1 [34].

The kinetics model confirms the extremely low yields of the chlorinated products determined by multipass infrared spectroscopy.

In an air stream of ∼30 L/min, with a methane concentration of 53±2 ppm, we have removed 58±4%

Table 1. Modelled concentrations of chlorocarbons.

Substance	Concentration [molecules/cm^3]	Product Yield [$\Delta X/\Delta CH_4$]	GWP_{20}
CH_4	5.1 (± 0.3) $\times 10^{14}$	0	79.7±25.8 [35]
CO	4.1 (± 0.1) $\times 10^{14}$	0.58	N/A
CO_2	1.0 (± 0.02) $\times 10^{16}$	0.37	1
CH_3Cl	7.2 (± 0.8) $\times 10^{10}$	1.0 $\times 10^{-4}$	45[36]
CH_2Cl_2	2.9 (± 0.4) $\times 10^{6}$	4.1 $\times 10^{-9}$	33[36]
$CHCl_3$	2.1 (± 0.3) $\times 10^{1}$	3.0 $\times 10^{-14}$	60[36]
CCl_4	1.9 (± 0.4) $\times 10^{-5}$	2.6 $\times 10^{-20}$	3480[36]

of the methane, by activating chlorine gas into chlorine radicals using 368 nm LEDs at a power of 110 W. The apparent quantum yield of MEPS was found to be 0.21-0.83%, with a specific energy input of 2.1-7.6 kWh/gCH_4 and volumetric energy input of 36-244 kJ/m^3 of air. Multiplying the carbon intensity of electricity of Norway, 29 gCO_2e/kWh [37], by the lowest specific energy input we achieved, 2.1 kWh/gCH_4, this implies a ratio of 61 gCO_2e/gCH_4 which is in the range of the 20 and 100 year GWP of CH_4, 82.5±25.8 and 29.8±11 respectively on a mass unit basis [35]. Clearly, electricity in most countries has a higher carbon intensity than in Norway and the calculation would need to be adjusted accordingly.

Abernathy et al.[17] found that light-based reactors must have a quantum yield for methane removal of at least 9±8%, in order for the economic benefit of removing methane to exceed the energy cost. Given the demonstrated performance of MEPS with an AQY of 0.83% and anticipated improvements, the possibility that MEPS will meet the target set by Abernathy et al. cannot be excluded.

4. Conclusion

MEPS, as described in this article, has been shown to effectively oxidize low-concentration methane in laboratory-scale experiments. Moreover, the process is easily controlled as the chlorine concentration and UV lights can be rapidly adjusted to match changes in pollution load. This technology is still under development and power efficiency is continually being improved, as described above. The technology is scalable and could eventually be deployed in a number of real-world scenarios. Further improvement in the chloride recycling system is also envisaged.

In the near future, the photoreactor will undergo field-testing at scale and once optimized, MEPS could be the first viable technology for direct oxidation of low-concentration point-source methane at scale. Perhaps with further improvements, MEPS would eventually be able to treat ambient concentrations of

methane when used in combination with a CO_2 DAC system.

Acknowledgments

The PERMA project is a collaboration between the University of Copenhagen, Aarhus University, Ambient Carbon ApS, Arla Foods, and Skov A/S to develop and field test a MEPS prototype. We thank these partners for their contributions to the PERMA project. We also thank NextGenerationEU and Innovation Fund Denmark for their Innomissions funding of the PERMA project under AgriFoodTure, and we thank AgriFoodTure for their administration in conjunction with the PERMA project. We would like to thank Bjørk Jakobsen for her help with methane measurements and Maarten van Herpen for helpful comments. We thank Ambient Carbon's David S. Miller and Laura LaCava for support and project management in conjunction with the research described in this article.

Data Availability Statement
The data gathered during experiments and the model used for examining the possibility of chlorocarbon formation, along with future removal scenarios, can be accessed by contacting the authors.

Author Contributions
MK and HSR conducted experiments and data analysis. All authors contributed to the development of the technique. All authors contributed to writing.

Conflict of interest
Ambient Carbon Methane Holding ApS owns patent WO2022053603A1(2022) [26].

References

[1] Harnung S E and Johnson M S 2012 *Chemistry and the Environment* (Cambridge University Press) ISBN 978-1-107-68257-3

[2] Arias P A, Bellouin N, Coppola E, Jones R G, Krinner G, Marotzke J, Naik V, Palmer M D, Plattner G K, Rogelj J *et al.* 2021 *IPCC AR6 WGI* p. 33–144(69) URL https://doi.org/10.1017/9781009157896.002

[3] Thoning K, Dlugokencky E, Lan X and NOAA Global Monitoring Laboratory 2022 Trends in globally-averaged ch4, n2o, and sf6 URL https://doi.org/10.15138/P8XG-AA10

[4] Szopa S, Naik V, Adhikary B, Artaxo P, Berntsen T, Collins W, Fuzzi S, Gallardo L, Kiendler-Scharr A, Klimont Z *et al.* 2021 *IPCC AR6 WGI* p. 853–4 URL https://doi.org/10.1017/9781009157896.008

[5] Saunois M, Stavert A R, Poulter B, Bousquet P, Canadell J G, Jackson R B, Raymond P A, Dlugokencky E J, Houweling S, Patra P K *et al.* 2020 *Earth System Science Data* **12** 1561–1623 URL https://doi.org/10.5194/essd-12-1561-2020

[6] Bonard A, Daële V, Delfau J L and Vovelle C 2002 *The Journal of Physical Chemistry A* **106** 4384–9 URL https://doi.org/10.1021/jp012425t

[7] Srinivasan N, Su M C, Sutherland J and Michael J 2005 *The Journal of Physical Chemistry A* **109** 1857–63 URL https://doi.org/10.1021/jp040679j

[8] Kirschke S, Bousquet P, Ciais P, Saunois M, Canadell J G, Dlugokencky E J, Bergamaschi P, Bergmann D, Blake D R, Bruhwiler L *et al.* 2013 *Nature Geoscience* **6** 813–23 URL https://doi.org/10.1038/ngeo1955

[9] Saiz-Lopez A and von Glasow R 2012 *Chemical Society Reviews* **41** 6448–72 URL https://doi.org/10.1039/C2CS35208G

[10] van Herpen M M J W, Li Q, Saiz-Lopez A, Liisberg J B, Röckmann T, Cuevas C A, Fernandez R P, Mak J E, Mahowald N M, Hess P, Meidan D, Stuut J B W and Johnson M S 2023 *Proceedings of the National Academy of Sciences* **120** e2303974120 URL https://doi.org/10.1073/pnas.2303974120

[11] Bryukov M G, Slagle I R and Knyazev V D 2002 *The Journal of Physical Chemistry A* **106** 10532–42 URL https://doi.org/10.1021/jp0257909

[12] Michelsen H A and Simpson W R 2001 *The Journal of Physical Chemistry A* **105** 1476–88 URL https://doi.org/10.1021/jp0016784

[13] Monai M, Montini T, Gorte R J and Fornasiero P 2018 *European Journal of Inorganic Chemistry* **2018** 2884–93 URL https://doi.org/10.1002/ejic.201800326

[14] Karacan C Ö, Ruiz F A, Cotè M and Phipps S 2011 *International journal of coal geology* **86** 121–56 URL https://doi.org/10.1016/j.coal.2011.02.009

[15] Gélin P and Primet M 2002 *Applied Catalysis B: Environmental* **39** 1–37 URL https://doi.org/10.1016/S0926-3373(02)00076-0

[16] Kwiatkowski S, Polat M, Yu W and Johnson M S 2021 *Air Pollution Sources, Statistics and Health Effects* 477–511 URL https://doi.org/10.1007/978-1-0716-0596-7_1083

[17] Abernethy S, Kessler M and Jackson R 2023 *Environmental Research Letters* URL https://doi.org/10.1088/1748-9326/acf603

[18] Yoon S, Carey J N and Semrau J D 2009 *Applied Microbiology and Biotechnology* **83** 949–56 URL https://doi.org/10.1007/s00253-009-1977-9

[19] Chen X, Li Y, Pan X, Cortie D, Huang X and Yi Z 2016 *Nature Communications* **7** 12273 URL https://doi.org/10.1038/ncomms12273

[20] Beauchemin K A, Ungerfeld E M, Abdalla A L, Alvarez C, Arndt C, Becquet P, Benchaar C, Berndt A, Mauricio R M, McAllister T A, Oyhantçabal W, Salami S A, Shalloo L, Sun Y, Tricarico J, Uwizeye A, De Camillis C, Bernoux M, Robinson T and Kebreab E 2022 *Journal of Dairy Science* **105** 9297–326 URL https://doi.org/10.3168/jds.2022-22091

[21] Jackson R B, Abernethy S, Canadell J G, Cargnello M, Davis S J, Féron S, Fuss S, Heyer A J, Hong C, Jones C D, Damon Matthews H, O'Connor F M, Pisciotta M, Rhoda H M, de Richter R, Solomon E I, Wilcox J L and Zickfeld K 2021 *Philosophical Transactions of the Royal Society A: Mathematical, Physical and Engineering Sciences* **379** 20200454 URL https://doi.org/10.1098/rsta.2020.0454

[22] Linstrom P and Mallard W Retrieved 22 august 2023 Nist chemistry webbook, nist standard reference database 69 URL http://doi.org/10.18434/T4D303

[23] Jessen C H, Bendix J, Nannestad T B, Bordallo H N, Pedersen M J, Pedersen C M and Bols M 2023 *New Journal of Chemistry* **47** 14624–9 URL https://doi.org/10.1039/D3NJ01843A

[24] Johnson M S and Arlemark J 2009 *World Intellectual*

Property Organization **WO2009138464A1**

[25] Johnson M S, Nilsson E J, Svensson E A and Langer S 2014 *Environmental Science & Technology* **48** 8768–76 URL https://doi.org/10.1021/es5012687

[26] Johnson M S, Schmidt J A and Pugliese S 2022 *World Intellectual Property Organization* **WO2022053603A1**

[27] Polat M, Liisberg J B, Krogsbøll M, Blunier T and Johnson M S 2021 *Atmospheric Measurement Techniques* **14** 8041–67 URL https://doi.org/10.5194/amt-14-8041-2021

[28] Burkholder J, Sander S, Abbatt J, Barker J, Cappa C, Crounse J, Dibble T, Huie R, Kolb C, Kurylo M *et al.* 2019 Chemical kinetics and photochemical data for use in atmospheric studies; evaluation number 19, jpl publication 19-5 Tech. rep. Pasadena, CA: Jet Propulsion Laboratory URL https://jpldataeval.jpl.nasa.gov/

[29] Manion J A, Huie R E, Levin R D, Jr D R B, Orkin V L, Tsang W, McGivern W S, Hudgens J W, Knyazev V D, Atkinson D B, Chai E, Tereza A M, Lin C Y, Allison T C, Mallard W G, Westley F, Herron J T, Hampson R F and Frizzell D H 2015 *NIST Standard Reference Database 17* **Version 7.0 (Web Version)** Data version 2015.09 URL https://kinetics.nist.gov/

[30] Prominent 2019 Assembly and operating instructions, chlorine electrolysis system chlorinsitu® iia, 625 ... 2,500 g/h URL https://www.prominent.com/resources/OperatingInstructions/English/24386/981413-BA-CI-019-12-19-EN-CHLORINSITU-IIa-625-2500-EN.pdf

[31] Luminus 2018 Sst-10-uv surface mount led URL https://download.luminus.com/datasheets/Luminus_SST-10-UV_Datasheet.pdf

[32] Jakobsen B 2023 *Evaluation of the Feasibility of a Low Cost Sensor for Methane* (University of Copenhagen) URL https://doi.org/10.17894/ucph.4c8d1adc-ffac-453f-b2c1-0ef7ebedc00a

[33] Claxton T, Hossaini R, Wild O, Chipperfield M P and Wilson C 2019 *Geophysical Research Letters* **46** 5489–98 URL https://doi.org/10.1029/2018GL081455

[34] *Handbook for the Montreal Protocol on Substances that Deplete the Ozone Layer* (United Nations Environment Programme (UNEP)) pp Section 1, p. 31 fourteenth(2020) ed

[35] Forster P, Storelvmo T, Armour K, Collins W, Dufresne J L, Frame D, Lunt D, Mauritsen T, Palmer M, Watanabe M, Wild M and Zhang H 2021 *IPCC AR6 WGI* p. 1017 URL https://doi.org/10.1017/9781009157896.009

[36] Myhre G, Shindell D, Bréon F M, Collins W, Fuglestvedt J, Huang J, Koch D, Lamarque J F, Lee D, Mendoza B, Nakajima T, Robock A, Stephens G, Takemura T and Zhang H 2013 *IPCC AR5 WGI* p. 731–3 URL https://www.ipcc.ch/report/ar5/wg1/

[37] Wiatros-Motyka M, Jones D, Broadbent H, Fulghum N, Bruce-Lockhart C, Dizon R, MacDonald P, Moore C, Candlin A, Lee U, Copsey L, Hawkins S, Ewen M, Worthingthon B, Benham H, Trueman M, Yang M, Lolla A, Edianto A S, Czyżak P, Brown S, Rosslowe C and Black R 2023 URL https://ember-climate.org/insights/research/global-electricity-review-2023/